

Modeling Ledger Dynamics in IOTA Blockchain

^{†‡}Fengyang Guo, [†]Xun Xiao, [†]Artur Hecker and [‡]Schahram Dustdar

[†]Munich Research Center, Huawei Technologies, Munich, Germany

[‡]Distributed Systems Group, TU Wien, Vienna, Austria

Abstract—IOTA blockchain is a new type of distributed ledger systems that is lightweight without mining and feeless-of-using. Rather than using a chain structure as in traditional blockchains, IOTA organizes ledger records with a directed acyclic graph (DAG), called *Tangle*. When message entries are committed into the ledger, the ledger tangle grows in a special way where multiple messages could be attached by different processing nodes in parallel. Such a unique evolution process motivates us to study the ledger tangle dynamics, which is unexplored so far. In this paper, we present the first generative modeling for IOTA tangle based on stochastic analysis. A key finding is that IOTA tangle renders a double Pareto Lognormal (dPLN) distribution, rather than typical network models (e.g., Power-Law and Exponential distributions). Quantitative comparisons show that the fitting quality of our model outperforms existing popular models on official real-world datasets published by IOTA Foundation. Estimated model parameters are provided, which is immediately instrumental for a more realistic IOTA network generator design. The proposed generative model also provides a deeper understanding of the internal mechanics of IOTA network.

Index Terms—IOTA Blockchain Network, Network Modeling, Network Dynamics, Degree Distribution

I. INTRODUCTION

In 2016, IOTA foundation (IF)¹ proposed a new type of blockchain—IOTA network. Instead of using a chain topology, IOTA uses a Directed Acyclic Graph (DAG), called *Tangle* topology, to organize ledger data on every processing node [1]. IOTA abandons proof-of-work (PoW) consensus and is feeless. Thus, IOTA is suitable for many IoT applications, where communications can be characterized as instant, massive exchange of tiny messages. Although IOTA enjoys a high popularity in research, most of the studies focus on statistical analysis [2], protocol extension/enhancement [3] and applications [4], [5]. In contrast, we would like to gain more insights into theoretical analysis, notably through network graph modeling, to reveal and better understand the core mechanism of IOTA network.

IOTA tangle evolves in a special way. Specifically, every vertex represents a single message record in the ledger (either a value transaction or a simple data payload). For a new message (e.g., submitted by a user), it will be attached as a new vertex with introducing new directed edges to existing vertices in the tangle. Semantically, each directed edge represents the approval from the source vertex (message) of the target vertex (message). Vertex selection is determined by specific *selection algorithms*, defined by the distributed consensus protocol. The key idea is to stimulate processing nodes attaching new

messages biasing on *tips*, i.e., vertices having no approver yet thus their in-degrees are zero. With the new vertices independently added in the tangle by different nodes, the size of the tangle will grow with multiple vertex- and edge-arrivals over time.

In this paper, we are interested in the tangle ledger dynamics driven by IOTA. It would be ideal to develop a formal network model capable of correctly describing the evolution of an operational IOTA tangle and in particular its stationary degree distribution. Alas, it appears unlikely that usual network models, e.g., random graphs [6]–[8] or the Barabási-Albert’s *Preferential Attachment* (PA) model [9] can correctly explain the IOTA tangle behavior. Key differences are as follows.

First of all, IOTA tangle typically grows non-uniformly, in bursts, during which multiple new vertices are added at the same time, each with more than one new edge. The reason for such bursts is tangle consolidation: since every node independently attaches incoming messages to its local tangle ledger copy, at one point, those individual tangles need to be consolidated and merged to one. During this phase, multiple messages and edges are added in one batch. In contrast, prior work usually assumes a single node arrival mode, and very often simplifies the process further to single edge addition. Hence, it is inaccurate to simplify IOTA tangle growing with a single vertex arrival mode.

Secondly, vertex and edge additions do not follow a simple PA model (or any of its variants). In PA model, a vertex is randomly selected proportionally to its degree. In IOTA, however, tip selection is a distributed decision-making process to identify a valid branch, where a new vertex can safely attach without causing conflicts. Such a process involves evaluating other existing vertices (i.e., historical messages) in a sub-tangle topology, thus it cannot be trivially abstracted as a simple vertex attribute (e.g., a degree value) as in PA model.

We will see that an alternative is required in order to derive a network model that can capture the essence of the ledger dynamics. In summary, the main contributions of this paper are as follows:

- We employ stochastic analysis to characterize IOTA tangle evolution with an Stochastic Differential Equation (SDE) that can approximately govern the vertex degree dynamics over time;
- We discover that operational IOTA tangles can be accurately described through the *double Pareto Lognormal* (dPLN) distribution;
- We quantitatively compare fitting quality of the proposed model against other popular candidate models with the

¹The official IOTA development and operation consortium

real-world data (whose size is around 320G) published by IOTA Foundation (IF). The results confirm the correctness of our key finding, where IOTA tangles render a dPLN degree distribution.

To the best of our knowledge, this is the first theoretical work modeling IOTA network dynamics. Estimated model parameters in this work are immediately instrumental for a more realistic IOTA network generator design.

The structure of this paper is outlined. We review existing network models in Section II and introduce IOTA preliminary as a background in Section III; Section IV presents our model and Section V introduces model fitting; after that Section VI shows the comparison results with existing popular models; Section VII concludes this paper.

II. RELATED WORK

Though there are very limited relevant theoretical works, we observed several attempts on analytical performance modeling about IOTA. In [10], [11], they built a rule-based discrete model and a continuous-time model for IOTA, respectively, in order to build the relationship of the number of tip vertices and the vertices' cumulative weights over time. In [12], the authors analyzed the message attachment behavior of IOTA network and proved that there exists a Nash equilibrium, revealing that selfish nodes will cost more than non-selfish nodes. This work targets to a different goal, which aims to theoretically model how the tangle topology evolves and what a degree distribution could best represent it.

The main difference of the IOTA network to random graph models summarized in [6] is that IOTA's ledger tangle is growing, while random graph models consider graph's size unchanged. This motivates us to consider those models characterizing evolving graph networks.

A famous growing/evolving network model (i.e., PA model) was proposed in [9]. In this model, new vertices attach to target vertices selected proportionally to their degree (often paraphrased as "rich gets richer"). The authors have shown that applying this simple principle results in a scale-free network, i.e., a graph with a Power-Law (PL) degree distribution). Hence, PA is a popular generator for (a particular class of) scale-free networks.

Cyclic PA (CPA) was introduced in [13] as a variant of the PA model. In CPA model, the attachment probability depends on the shortest path from the node to all other nodes. The author used this model to analyze the real world network, such as online social networks and relations amongst company leaders. The finding is that the proposed CPA provides more flexibility to model the real life networks. Additionally, [14] proposed another PA model variant to model a phenomenon, where a vertex acquires a new vertex depending on the density of its local area in a graph. Authors analytically obtain stable degree distributions and cluster in-degree correlations. They show the emergence of a Power-Law (PL) distribution of the resulting graph's degrees.

Although PA-like models provide decent modeling for a large number of evolving networks, the message attachment

in IOTA behaves differently. One key difference is that most of PA models only consider a single vertex arrival mode, while IOTA tangle grows with a batch arrival mode. Another key difference is that the attachment probability is determined by running an algorithm applied on a sub-tangle topology, which cannot be written in an analytical form as in PA models.

In reality, many phenomena are not following PA models. Their degree distributions are also not Power-Law (PL)/Exponential (Exp) distributions. For example, the authors showed respectively that the file size [15], the city size [16] and mobile call graphs [17] follow dPLN distributions [18]. Compared to them, the IOTA network is a distributed system and ledger dynamics are implicit. Hence, a correct modeling is required.

III. IOTA PRELIMINARY

We here briefly introduce how IOTA works for a better readability. IOTA is a distributed system consisting of processing *nodes*, each of which maintains a full ledger in a tangle structure. Every node has two main tasks: 1) attaching messages into its tangle and 2) propagating new messages to other nodes, forming a distributed consensus.

A. Message Attachment

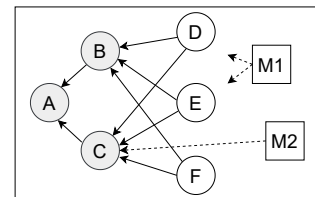


Fig. 1: Message attachment on one node

A new message is submitted by a client to a node. After an initial check (such as signature, balances and so on), the message will be attached to one or more existing vertices in the tangle (e.g., 'M1' and 'M2' in Fig. 1). In IOTA, semantically, an attachment corresponds to an "approval" of the information contained in the message that the new message attaches to and is part of the consensus mechanism: the more vertices attach to a given vertice (directly, or to its referrers), the higher the confidence in the information that this vertex bears.

Hence, the selection of vertices is of utmost importance. IOTA protocol always chooses among the *tips*, i.e., from the vertices with in-degree equal 0 (e.g., 'D', 'E' and 'F' in Fig. 1). The motivation behind this mechanism is to make every node contribute to the IOTA network by approving "younger" messages. In IOTA, every node has a *Tip Selection Algorithm* (TSA) module dedicated to this task. Although the exact TSA algorithms differ in IOTA 1.0 and 2.0, their outcomes for IOTA ledger dynamics are the same in the sense that both probabilistically select among the tips.

In principle, it is also possible to select other vertices for attachment. For example, a node could also attach to a message of a non-tip vertex (e.g., 'M2' could attach to 'C' in Fig. 1).

Attaching to such messages is safer because they are already approved and will not “disappear” as part of potential conflict resolution during tangle consolidation; in addition, depending on how the others select vertices (and the protocol version), later it might also be faster to get approved.

B. Tangle Consolidation and Consensus

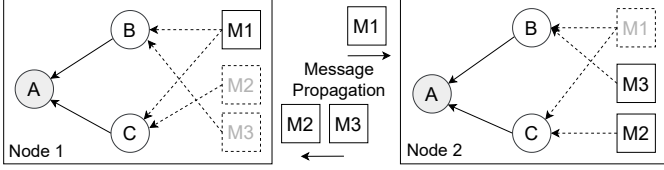


Fig. 2: Tangle consolidations

As nodes own local ledger copies, their views differ. Hence, tangle consolidation aims to propagate messages across the network so that tangle copies converge (see in Fig. 2, where ‘Node 1’ and ‘Node 2’ propagate local messages to each other). If the forwarded message exists, the node ignores it but forwards to other neighbors (except to the expedient); otherwise, a node saves the message and checks, if its two referenced messages can be found locally; if so, the message is merged into the local tangle; if missing, the message is suspended, until all missing messages are found by sending message requests recursively to neighbors.

Since distributed consensus is an intermediate phase before a tangle actually grows, it does not fundamentally alter the manner of network dynamics. In fact, message attachment already takes the outcome of a distributed consensus into consideration.

In summary, the key idea behind IOTA is that new messages approve old messages. Attached messages will be propagated across the whole network, thus tangles converge and consensus opinions are formed with a distributed consensus protocol. For more information, please refer to the IOTA protocol specifications [19].

IV. IOTA TANGLE LEDGER DYNAMICS

A. Key Idea

We denote a subset of vertices in a tangle where all vertices have the same degree $k \in \mathbb{Z}^+ \cup \{0\}$ as $G_k(t)$ at time t , called a *degree group*. The cardinality (size) of a degree group is $|G_k(t)| = s_k(t)$, called *Degree Group Size* (DGS). Let us further denote all new edges, which are added from several new messages to the same vertex, as e_t , called an *edge group*. In IOTA network, $s_k(t)$ can change because of the following two ways as illustrated in Fig. 3.

The first way is that $s_k(t)$ increases, because there could be one or more vertices, whose original degrees are less than k but an edge group e_t makes the degree increase to k by adding $|e_t|$ new edges. V_a in Fig. 3 is such an example, where V_a joins in degree group $G_k(t)$ and increases $s_k(t)$ by one.

The second way is that $s_k(t)$ decreases, because there could be a vertex, whose degree is already k , but another edge group

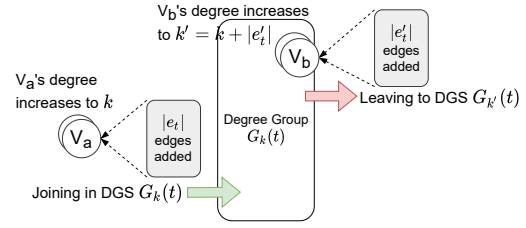


Fig. 3: Dynamics of DGS $s_k(t)$ of $G_k(t)$

e'_t makes its degree increase to k' by adding $|e'_t|$ new edges. V_b in Fig. 3 is an example, where V_b leaves to degree group $G_{k'}(t)$ and decreases $s_k(t)$ by one.

Mapping to IOTA network, the first situation happens to any vertex with a degree value between $[0, k)$, and the second situation happens to any vertex with a degree value is equal to k , thus covering all types of vertices in a tangle. For instance, a tip vertex (i.e., degree value is 0) will join in degree group $G_k(t)$, if an edge group e_t adds exactly k edges to it (i.e., $|e_t|$ is k); any non-tip vertex whose degree is $< k$ will also join in degree group $G_k(t)$ if an edge group e_t adds up its degree value to k . However, attaching to any vertex, whose degree is already k will make the vertex leave the degree group $G_k(t)$. All vertex selection cases are introduced in Section III-A.

From a statistical view, the macro effect of the joining and leaving vertices of a degree group $G_k(t)$ can be viewed as a Brownian motion [20], because how DGS $s_k(t)$ will exactly change is a stochastic process, which is driven by the random behaviors (e.g., random vertex selections) from processing nodes in IOTA blockchain.

B. A Stochastic Model

Considering the above two possible ways $s_k(t)$ may change, the ratio of the variation of $s_k(t)$ to its original value $s_k(t)$ can be either positive, zero or negative. Mathematically, it can be formulated with a Stochastic Differential Equation (SDE) of DGS $s_k(t)$ as follows.

$$\frac{ds_k(t)}{s_k(t)} = \omega(t)dt + \sigma(t)dB(t), \quad (1)$$

where $\omega(t)$ and $\sigma(t)$ are coefficients characterizing the growth rate of DGS and the variation of DGS resulting from random selection behaviors, which is modeled as a Brownian motion $dB(t)$. Another implicit necessity is that $s_k(t)$ must be a non-negative value. However, if we directly model the amount change of $s_k(t)$ (rather than the ratio $\frac{ds_k(t)}{s_k(t)}$ as in Eq. (1)), the Brownian motion term may lead to $s_k(t)$ becoming negative, which would contradict its definition.

The SDE in Eq. (1) agrees the form of Geometric Brownian Motion (GBM), which is analytically solvable if $\omega(t)$ and $\sigma(t)$ are time independent. Interested readers are referred to [21] for the details of deriving GBM’s theoretical properties. Here we recap them as follows:

- 1) The solution of the SDE of $s_k(t)$ in Eq. (1):

$$s_k(t) = s_k(0) \exp \left\{ \underbrace{\left(\omega - \frac{\sigma^2}{2} \right) t + \sigma B_t}_{\text{Denoted by } \mu} \right\}, \quad (2)$$

where the μ term is used in the following equations.

- 2) The *Probability Density Function* (PDF) of $s_k(t)$ at any observation time t follows a Lognormal (LN) distribution:

$$p_{\text{LN}}(x, t) = \frac{1}{x\sigma\sqrt{2\pi t}} \exp \left\{ -\frac{(\log x - t\mu)^2}{2t\sigma^2} \right\}. \quad (3)$$

- 3) The PDF of $s_k(t)$ at an exponentially distributed observation time t (i.e., $p_T(t) = \xi e^{-\lambda t}$) follows a dPLN distribution:

$$p_{\text{dPLN}}(x) = \frac{\alpha\beta}{\alpha + \beta} \left[x^{-\alpha-1} A(\alpha) \Phi \left(\frac{\log x - \mu - \alpha\sigma^2}{\sigma} \right) + x^{\beta-1} A(-\beta) \Phi^c \left(\frac{\log x - \mu + \beta\sigma^2}{\sigma} \right) \right], \quad (4)$$

where $A(z) = \exp(z\mu + \alpha^2\sigma^2/2)$, $z = \{\alpha, -\beta\}$, $\Phi(\cdot)$ and $\Phi^c(\cdot)$ are the Cumulative Density Function (CDF) and complementary CDF of a standard normal distribution, respectively. The model parameters of a dPLN distribution are $\theta := [\mu, \sigma^2, \alpha, \beta]$, which will be estimated from observed data.

The interpretation to our problem is that the DGS $s_k(t)$ grows along with the tangle over time t and the stoppage time t is assumed exponentially distributed. Importantly, the PDF in Eq. (4) tells what the probability density size of a certain degree group $G_k(t)$ will be. After normalized with the total tangle size n , it tells exactly the *degree distribution* of a tangle that we target.

V. MODEL FITTING

A. Fitting Data Preparation

We use real ledger data generated from IOTA mainnet on Internet that are published by IF². The whole dataset contains ledger records from 2016.11-2019.06 (Period I) and 2020.04-2020.08 (Period II). Period I contains 96 tangles and Period II contains 16 tangles (112 tangles in total). The number of messages of reconstructed tangles vary from several thousands to about 40 millions. To prepare the data for model fitting, there are two main challenges when processing the original datasets as follows.

The first challenge is that the published ledger data is represented in trytes but compressed in bytes. Thus, decompression and data format conversion have to be done at the first place. After the conversion, the datasets are converted into human-readable format and saved as JSON files.

The second challenge is that tangle topology information is not explicitly recorded. This means that tangle topology has to be reconstructed manually. We iterate all message records to identify their edges and connected vertices according to

the hash values of the two referenced messages. A more challenging case is that multiple tangles could exist in one batch. This further requires us to cluster messages manually that belong to the same tangle by identifying individual genesis vertices and the last vertices attached to the tangle starting from a particular genesis.

After all tangles are reconstructed, the vertex's (in-)degree value is calculated by summing up the total number of attached messages of the considered vertex. For a certain degree group G_k , its DGS s_k is the number of vertices having the same degree k in the tangle. For each vertex in $G_k, \forall k \in [1, K]$, the observed probability (proportion) of such a degree group $y_i = \frac{s_k}{n}$. This thus gives the fitting data for the proposed model.

B. Model Parameter Estimation

Maximization Likelihood Estimation (MLE) is a general method of estimating the parameters of an assumed probability distribution model, given observed data. Mathematically, this is achieved by maximizing the likelihood of observed data \mathcal{Y} with an presumed parametric model characterized by parameter θ . Specifically, we have:

$$\theta^* \leftarrow \arg \max_{\theta} \ell_{\text{PDF}}(\theta; \mathcal{Y}), \quad (5)$$

where the $\ell_{\text{PDF}}(\cdot)$ is the log-likelihood function defined as follows:

$$\ell_{\text{LP}}(\theta; \mathcal{Y}) = \sum_{i=1}^n \log f_{\text{PDF}}(\theta; y_i), \quad (6)$$

where $f_{\text{PDF}}(\cdot)$ is the PDF of the presumed model. For example, it can be dPLN model's PDF Eq. (4), or any other candidate models.

To solve Eq. (5), in the simplest cases, where an analytical solution of the optimal estimate exists, the optimal estimate can be obtained directly. This situation exists to most of simple statistical models such as PL and Exp distributions and so on. In difficult cases, where the analytical solution does not exist, solving MLE needs numerical algorithms. Since the fitting algorithm is not the main focus of this work, we follow the MLE formulation and use an optimizer 'L-BFGS-B', which is a classical gradient-descent method proposed in [22], to solve the MLE problem in Eq. (5). Note that this routine is commercialized and directly available in Python library.

Note that though MLE is a principal way to handle the parameter estimation problem, the key issue of using MLE is that the likelihood function is usually not convex or concave (due to the sum of a number of log-PDF terms). Hence, whether or not the estimated parameter is a global optimum is uncertain. In fact, there are rich research topics on non-linear optimization, which is also planned as our future work for studying the efficiency of dPLN's parameter estimation.

VI. RESULTS

A. Candidate Models and Scoring Metrics

The candidate models for comparisons and their parameter estimations are summarized in Table I. The model complexity increases from PL and Exp to LN and dPLN. The number of

²<https://dbfiles.iota.org/>

Model	PDF	Model Parameters	MLE Solution
PL	$\zeta x^{-\gamma}$	γ	Closed-Form
Exp	$\xi e^{-\lambda x}$	λ	Closed-Form
LN	Eq. (3)	μ, σ^2	Closed-Form
dPLN	Eq. (4)	$\mu, \sigma^2, \alpha, \beta$	L-BFGS-B

TABLE I: Summary of candidate models (ζ and ξ : Normalization Constants)

model parameters also increases from 1 to 4, thus becoming reasonably representative for both model performance and complexity.

We choose Root Mean Squared Logarithmic Error (rMSLE) to measure the fitting quality of different models. Its definition is given below:

$$\text{rMSLE} = \sqrt{\frac{1}{n} \sum_{i=1}^n (\log y_i - \log \hat{y}_i)^2}, \quad (7)$$

where n is the total number of observed vertices, and \hat{y}_i is the predicted probability value of observed probability value y_i . rMSLE measures the *relative errors* of the predicted and actual values. The reason to choose rMSLE is that the probabilities between different types of vertices may be significantly different with several magnitudes. In this case, unit dependent measures e.g. MAE (Mean Square Error) turns out to be unsuitable because the absolute distances of errors from data points with smaller proportions will be overwhelmed. rMSLE solves this issue so that it becomes unit independent by taking a log-difference/relative ratio.

B. Quantitative Fitting Comparison

Fig. 4 shows the four candidate models' performance scored by rMSLE on different parts of the vertex population. The optimal rMSLE is 0 highlighted with a yellow bar, meaning all observed and predicted data exactly match.

On the overall interval (Fig. 4a), the rMSLE mean of dPLN model is 0.3. LN model is at the second place but its rMSLE mean is about 0.5, which is worse than dPLN model's. Both Exp and PL are incorrect models to explain the observed in-degree distributions of the tangle snapshots with much larger rMSLEs.

On segmented parts, in the head and middle parts, LN model performed slightly better than dPLN model (see Fig. 4b and Fig. 4c). However, the rMSLE mean shown by two models are actually quite close to each other, especially the median rMSLE. Neither Exp nor PL models fits these two parts well, especially in the head part. In the rear part (see Fig. 4d), the best is dPLN model. Surprisingly, the performance of LN model degrades significantly, although it performs well on the previous two intervals even slightly wins against dPLN model.

As we know, the uniqueness of a population is determined by the minority instead of majority features. The segmented comparisons above justify this fact because although a candidate model can perform better to some common features, its overall performance can still be hindered. For example, LN

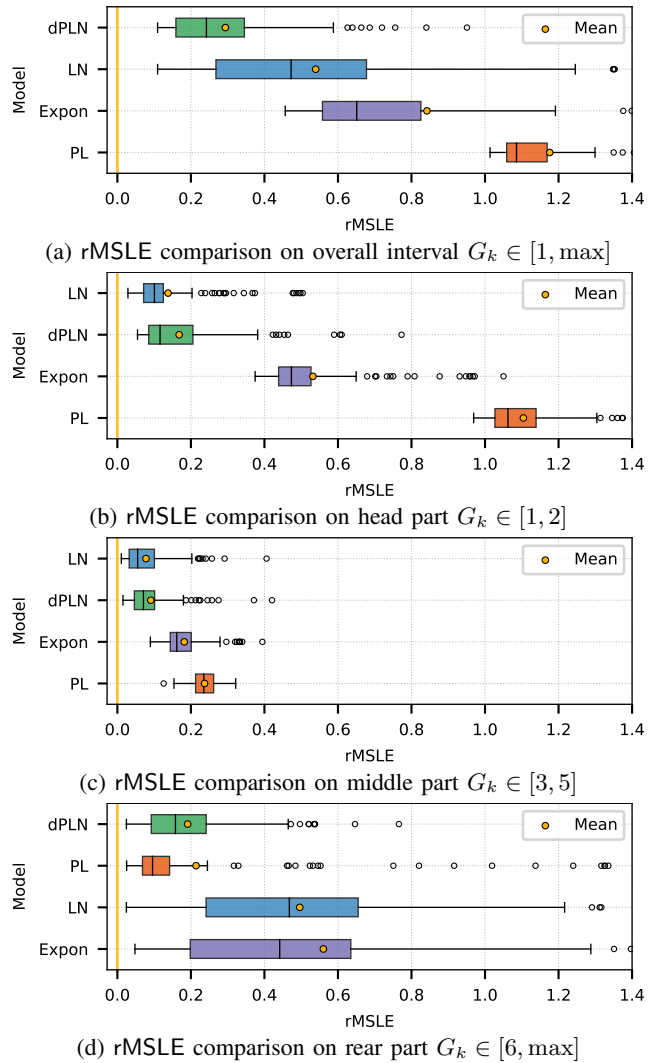


Fig. 4: Comparisons of candidate models with rMSLE

model strongly biases to fit vertices in the head and middle parts, in which both are majority. However, LN model completely ignores the minority feature of higher degree vertices in the tangles. Although the proportion of high degree vertices is small, a significant divergence on them failed LN model's overall performance. In contrast, only dPLN model showed a good balance between majority and minority features, which explains why it can eventually achieve an overall quality fitting results.

We also provide the estimated values of model parameters in Section VI-B. These values can be directly used with our model to generate tangles that give the most realistic topology as in IOTA mainnet.

C. Graphical Fitting Comparison

We then provide a graphical comparison of the candidate models with three tangle examples in Fig. 5. This helps readers to capture the difference of model performances in a visual way. For fairness, we pick the three tangle samples with

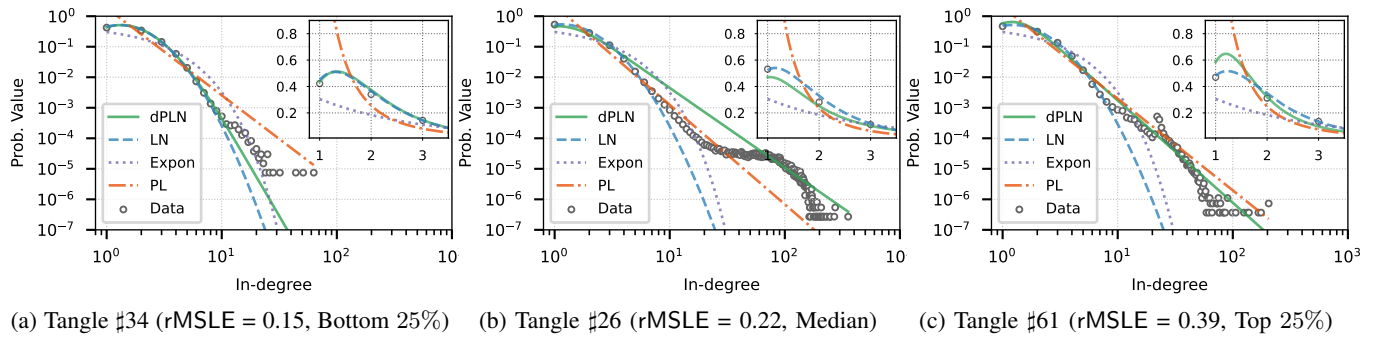


Fig. 5: Graphical fitting comparison

Parameters	μ	σ^2	α	β
Mean	0.29	0.15	17.00	14.92
Variance	0.03	8e-3	517.93	185.28
1/4 Quartile	0.16	0.09	2.32	5.01
Median	0.32	0.18	3.17	9.65
3/4 Quartile	0.44	0.21	36.21	27.72

TABLE II: Statistics of estimated model parameters

top 25%, median and bottom 25% rMSLEs of dPLN model, respectively. We also zoom in the fitting of degree group [1, 3] in the subplots at the upper right corner.

Generally, the graphical fittings match the quantitative results. Specifically, dPLN model (green-solid curves) fits averagely closer to the observed distributions in all parts. Additionally, LN model fits slightly better to the head part but extremely poorer in the rear part. As we can see, it diverts the farthest to the tails. Moreover, none of PL and Exp models is a reasonable choice.

In summary, the evaluation results can tell that with the real-world data from IOTA mainnet, the network dynamics result in a dPLN distribution, which invalidates the typical assumption of either PL or Exp models in this space.

VII. CONCLUSION

In this paper, we modeled IOTA ledger dynamics with stochastic analysis and analytically derived its degree distribution. Our key finding is that the tangle topology of IOTA network renders a dPLN distribution. This finding was confirmed by fitting our model predictions to official datasets and the proposed model outperforms other existing models. We hope that this promotes a deeper understanding of the mechanism of IOTA and hence benefit IOTA network generator design for further research and/or application purposes.

REFERENCES

- [1] S. Popov, "The tangle," *cit. on*, p. 131, 2016.
- [2] C. Fan, H. Khazaei, Y. Chen, and P. Musilek, "Towards A Scalable DAG-based Distributed Ledger for Smart Communities," in *2019 IEEE 5th World Forum on Internet of Things (WF-IoT)*. IEEE, 2019, pp. 177–182.
- [3] P. Perazzo, A. Arena, and G. Dini, "An analysis of routing attacks against iota cryptocurrency," in *2020 IEEE International Conference on Blockchain (Blockchain)*, 2020, pp. 517–524.
- [4] P. C. Bartolomeu, E. Vieira, and J. Ferreira, "Tota feasibility and perspectives for enabling vehicular applications," in *2018 IEEE Globecom Workshops (GC Wkshps)*. IEEE, 2018, pp. 1–7.
- [5] X. Xiao, F. Guo, and A. Hecker, "A lightweight cross-domain proximity-based authentication method for iot based on iota," in *2020 IEEE Globecom Workshops (GC Wkshps)*, 2020, pp. 1–6.
- [6] X. Zhang, C. Moore, and M. E. J. Newman, "Random graph models for dynamic networks," *The European Physical Journal B*, vol. 90, no. 10, p. 200, Oct. 2017. [Online]. Available: <http://link.springer.com/10.1140/epjb/e2017-80122-8>
- [7] W. Aiello, F. Chung, and L. Lu, "A random graph model for power law graphs," *Experimental Mathematics*, vol. 10, no. 1, pp. 53–66, 2001.
- [8] D. Garlaschelli, "The weighted random graph model," *New Journal of Physics*, vol. 11, no. 7, p. 073005, 2009.
- [9] A.-L. Barabási and R. Albert, "Emergence of scaling in random networks," *science*, vol. 286, no. 5439, pp. 509–512, 1999.
- [10] B. Kusmierz, "The first glance at the simulation of the tangle: discrete model," *IOTA Found. WhitePaper*, pp. 1–10, 2017.
- [11] B. Kusmierz, P. Staube, and A. Gal, "Extracting tangle properties in continuous time via large-scale simulations," *Technical Report. working paper*, pp. 2018–08, 2018.
- [12] S. Popov, O. Saa, and P. Finardi, "Equilibria in the tangle," *Computers & Industrial Engineering*, vol. 136, pp. 160–172, Oct. 2019. [Online]. Available: <https://www.sciencedirect.com/science/article/pii/S0360835219304164>
- [13] D. Kasthurirathna and M. Piraveenan, "Cyclic preferential attachment in complex networks," *Procedia Computer Science*, vol. 18, pp. 2086–2094, 2013.
- [14] L.-N. Wang, J.-L. Guo, H.-X. Yang, and T. Zhou, "Local preferential attachment model for hierarchical networks," *Physica A: Statistical Mechanics and its Applications*, vol. 388, no. 8, pp. 1713–1720, 2009.
- [15] M. Mitzenmacher, "Dynamic models for file sizes and double pareto distributions," *Internet Mathematics*, vol. 1, no. 3, pp. 305–333, 2004.
- [16] K. Giesen, A. Zimmermann, and J. Suedekum, "The size distribution across all cities—double pareto lognormal strikes," *Journal of Urban Economics*, vol. 68, no. 2, pp. 129–137, 2010.
- [17] M. Seshadri, S. Machiraju, A. Sridharan, J. Bolot, C. Faloutsos, and J. Leskovec, "Mobile call graphs: beyond power-law and lognormal distributions," in *Proceedings of the 14th ACM SIGKDD international conference on Knowledge discovery and data mining*, 2008, pp. 596–604.
- [18] W. J. Reed and M. Jorgensen, "The double pareto-lognormal distribution—a new parametric model for size distributions," *Communications in Statistics-Theory and Methods*, vol. 33, no. 8, pp. 1733–1753, 2004.
- [19] W. F. Silvano and R. Marcelino, "Iota tangle: A cryptocurrency to communicate internet-of-things data," *Future Generation Computer Systems*, vol. 112, pp. 307–319, 2020.
- [20] E. Nelson, *Dynamical theories of Brownian motion*. Princeton university press, 2020.
- [21] I. Karatzas and S. Shreve, *Brownian motion and stochastic calculus*. Springer Science & Business Media, 2012, vol. 113.
- [22] C. Zhu, R. H. Byrd, P. Lu, and J. Nocedal, "Algorithm 778: L-BFGS-B: Fortran subroutines for large-scale bound-constrained optimization," *ACM Transactions on Mathematical Software*, vol. 23, no. 4, pp. 550–560, Dec. 1997.